Plasma electrostatic turbulence in TCV tokamak edge: direct comparison of experiment with 2D simulation

J. Horacek[1], O.E.Garcia[2], J.P.Graves[1], R.A.Pitts[1], A.H.Nielsen[2], V.Naulin[2], J.J.Rasmussen[2]

[1] *Centre de Recherches en Physique des Plasmas, EPFL, Lausanne, Switzerland*
[2] *Association EURATOM-Risø National Laboratory, Roskilde, Denmark*

Introduction

Experimentally, radial transport in the tokamak scrape-off layer (SOL) has long been measured to occur at anomalously high rates [1], often $100-1000\times$ faster than expected on the basis of collisional, non-turbulent diffusion [2]. Nowadays the transport is believed to occur through convection in the form of coherent structures (blobs) which propagate radially through the SOL. Charge separation inside the blobs, caused by magnetic guiding center drifts, leads to a poloidal electric field and thus a radial advection due to the corresponding electric drift. This contribution presents a comparison between measurements of electrostatic turbulence in the TCV SOL with the results of two-dimensional fluid turbulence simulations and will show for the first time that much of the statistical character seen in experiment can be quantitatively captured by theory throughout the SOL.

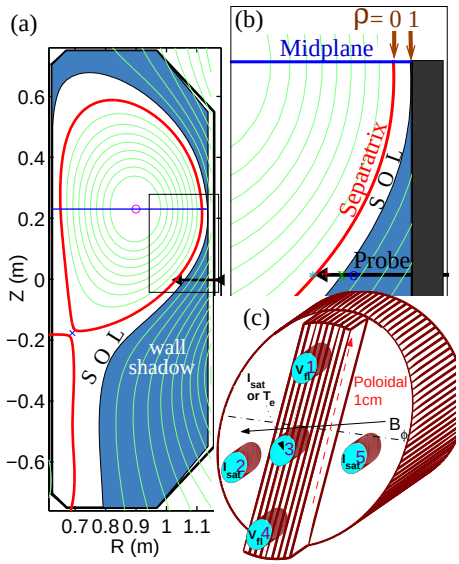

Figure 1: **(a)** Poloidal cross-section of TCV discharge #24530, enlarged in **(b)** showing the normalized coordinate, ρ. The probe head is shown schematically in **(c)**.

Experimental measurements on the TCV tokamak are obtained using a reciprocating Langmuir probe that enters the plasma on the outside machine midplane (Fig. 1ab). During a single reciprocation, the probe travels first through the "wall shadow", before encountering the main SOL region on field lines connecting to the divertor targets and then finally crossing the separatrix to enter the confined plasma. The density, n_e, is obtained from the ion saturation current, $I_s \propto n_e\sqrt{T_e}$ sampled at $6MHz$, but since the electron temperature, T_e is measured at $1kHz$ only, relative T_e fluctuations must be assumed small.

The ESEL model

The ESEL (Edge-SOL Electrostatic) code [3] solves a reduced fluid 2D model for self-consistent time evolution of edge plasma fluctuations. The turbulence is driven by the interchange mode arising as a consequence of the inhomogeneous magnetic field. Linear damping of all fields is provided by parallel particle losses in the SOL. The governing equations describe the evolution of n_e, T_e and plasma vorticity, $\Omega \stackrel{\text{def}}{=} \vec{\nabla}\times\vec{v}$ in a quasi-symmetric form [3]:

$$\frac{dn_e}{dt} + n_e\mathscr{C}(\phi) - \mathscr{C}(n_eT_e) = \Lambda_n\ ,\quad \frac{d\Omega}{dt} - \mathscr{C}(n_eT_e) = \Lambda_\Omega$$

$$\frac{dT_e}{dt} + \frac{2T_e}{3}\mathscr{C}(\phi) - \frac{7T_e}{3}\mathscr{C}(T_e) - \frac{2T_e^2}{3n_e}\mathscr{C}(n_e) = \Lambda_T$$

where the vorticity is related to the electrostatic potential through $\Omega = \nabla_\perp^2 \phi$. Time is normalized to the ion Larmor frequency $t \to t\omega_{ci}$ ($\approx 60MHz$ under TCV conditions) and the spatial coordinates $x = \rho/\rho_{iL}$ (radial) and $y = Z/\rho_{iL}$ (poloidal) are in units of the hybrid thermal ion Larmor radius, $\rho_{iL} \approx 0.7mm$ at the LCFS. The model geometry is illustrated in Fig. 2a together with the boundary conditions which has been modified with respect to [3]. The advective time derivative

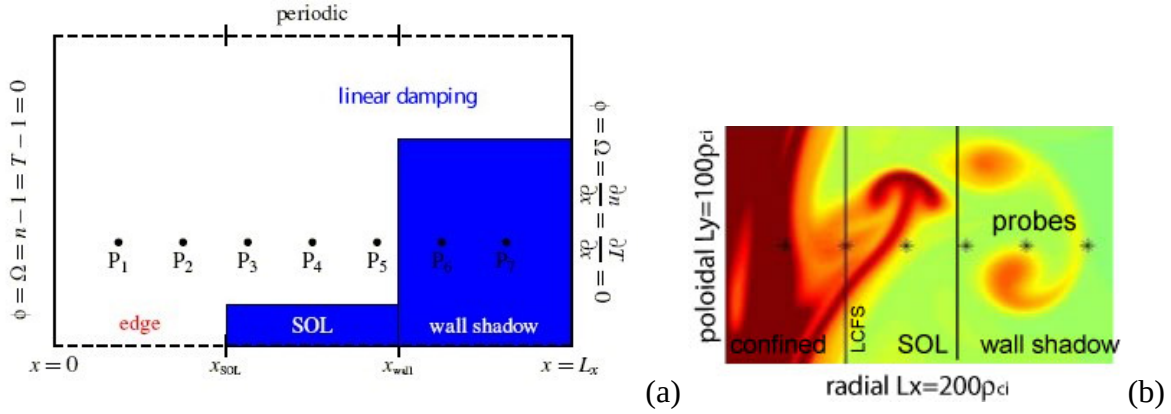

Figure 2: (a) ESEL code input geometry depicting position of the probes *$P_\#$, boundary conditions and regions of confinement and damping. (b) Example of ESEL output showing the formation and propagation of density blobs.

and the magnetic field curvature operator are defined as $\frac{d}{dt} \stackrel{\text{def}}{=} \frac{\partial}{\partial t} + B^{-1}\vec{z} \times \nabla\phi \cdot \nabla, \quad \mathscr{C} \stackrel{\text{def}}{=} -\zeta \frac{\partial}{\partial y}$. The influence of sinks, sources and dissipation is described as $\Lambda_n = D_n \nabla_\perp^2 n - \sigma_n n$ where D_n is the collisional diffusion coefficient and σ_n represents particle losses due to transport along open magnetic field lines in the SOL. Analogous quantities Λ_T and Λ_Ω are defined for the temperature and vorticity respectively. The values of the diffusion coefficients are free input parameters and are adjusted, within realistic margins, by comparison of the statistical analysis of code output with that performed on the experimental data. The following normalizations are used in the model: $n_e \to n_e/n_0$ and $T_e \to T_e/T_0$; the magnitude of n_0, T_0 is present only indirectly through value of diffusion coefficients. Ionization, parallel dynamics (flows and currents) and finite ion Larmor radius are neglected. An example of the model output illustrating the formation and propagation of 2D structures is shown in Fig. 2b.

Model-Experiment comparison

Statistical analysis on time-sequences of 5 ms duration is performed for both experiment and model in exactly the same way. Ref. [4] describe in more detail the methodology of this analysis with respect to TCV data. The main statistical characteristics are compared in Fig. 3 for TCV discharge #24530 at low and high density and the ESEL run with $D_\Omega/3 = D_n = D_T = 0.01$. Fig. 3ad contains several important features: the radial density gradient in code and experiment are in reasonable agreement and the absolute values of the inverted relative fluctuation level, $A = \langle n_e \rangle / \sigma_n$ are comparable over the entire radial region over which experimental data exist, where $\langle n_e \rangle$ is the time-averaged density and σ_n the standard deviation. The level of intermittency increases with distance into the SOL, particularly in the wall shadow where code results are available in regions where the experimental signal level is too low for reliable measurements. The shape of the density probability distribution function (PDF) is quantified by the Skewness, S and Kurtosis, K parameters, allowing straightforward comparison with known analytical distribution functions. As shown clearly in Fig. 4, the Gamma distri-

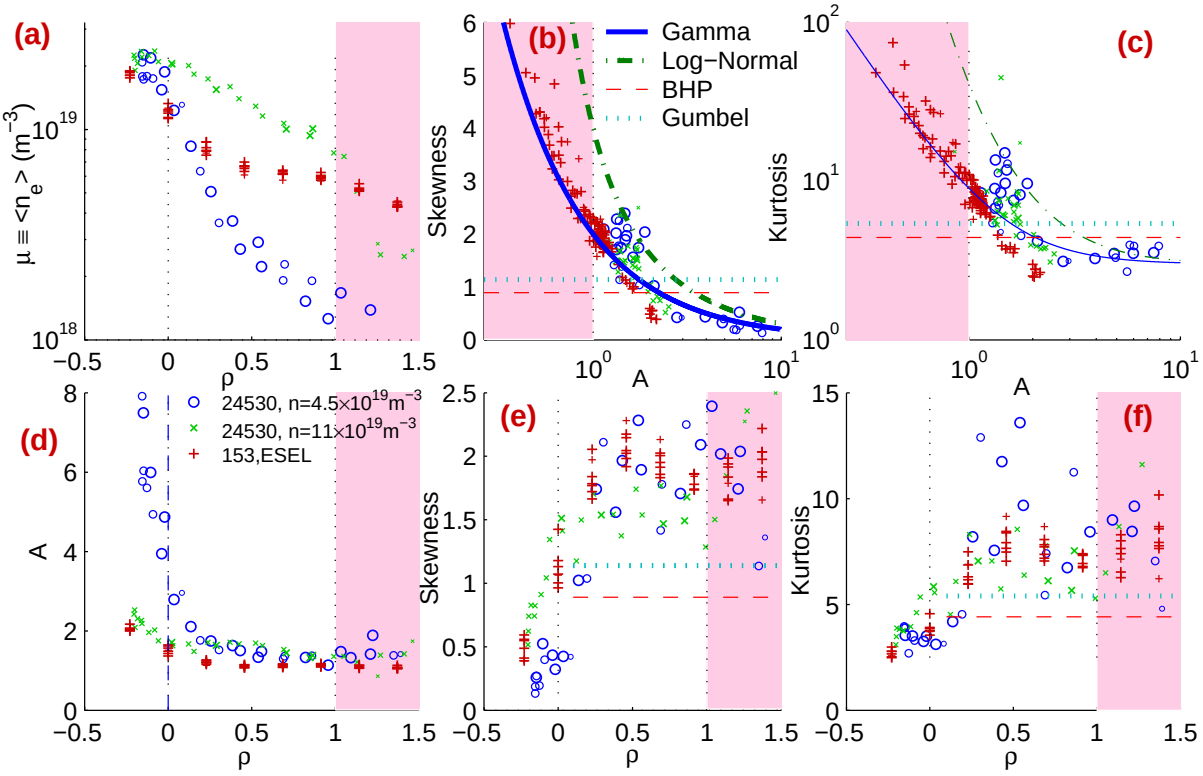

Figure 3: Variation with respect to normalized probe position (ρ) of the local density **(a)**, inverted relative fluctuation level $A = \mu/\sigma$ **(d)**, Skewness **(e)** and Kurtosis **(f)**. Further, Skewness **(b)** and Kurtosis **(c)** as a function of A in comparison with various statistical distributions. Note that $A < 1$ corresponds to the deep wall-shadow ($\rho > 2$) which is experimentally inaccessible and therefore not shown in **a,d,e,f**.

bution [5] is an excellent descriptor of both experiment (see also [4]) and model, thus indicating that both conform to the same statistical process. This is illustrated also in Fig. 3bc by the good fit of S(A) and K(A) to the code and TCV data, where $S = 2/A$ and $K = 3 + 6/A^2$ for the Gamma distribution. A close relative of the Gamma distribution is the Log-normal distribution [5] which has been found to reasonably match experimental density PDF's, in this time in a reversed field pinch [6]. It also provides a good match to the TCV data in the wall shadow, but performs less well than the Gamma distribution across the entire SOL width and does not compare favorably at all with the ESEL model. The Log-normal skewness and kurtosis are defined as [5] $S = 3/A + A^{-3}$, $K = \lambda^4 + 2\lambda^3 + 3\lambda^2 - 3$, where $\lambda \equiv 1 + A^{-2}$.

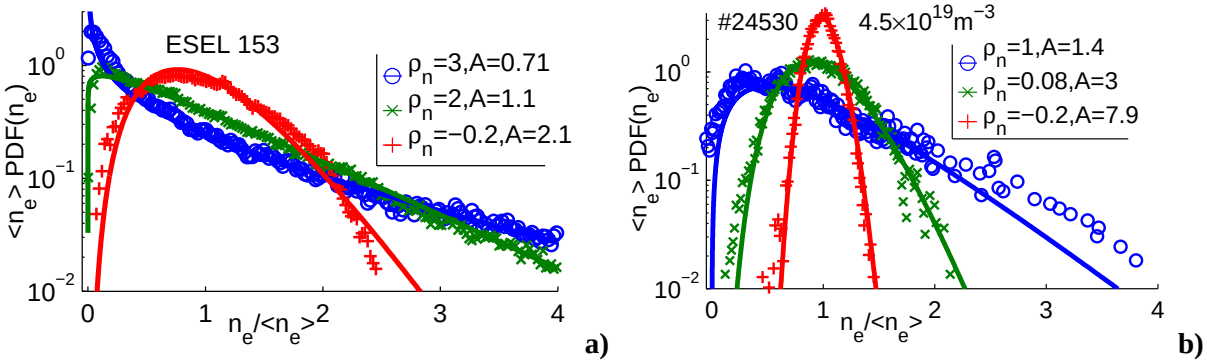

Figure 4: Both ESEL model (**a**) and TCV (#24530, **b**) PDF's conform well to the Gamma distribution.

A number of fixed shape distributions may also be compared with the data: the Gaussian (S=0, K=3), Gumbel (S=1.14, K=5.4) [7] and the BHP (S=0.89, K=4.415) [8] distributions. Fig. 3bc clearly shows that neither TCV nor ESEL data can be described by any fixed-shape PDF, in contrast to the recent observation in [9] that electrostatic turbulence statistics tend towards the universal BHP distribution. Rather, the density fluctuations appear to be a member of a family of intermittent systems which conform to a Gamma process. In addition to the example discharge (#24530) used here for model-experiment comparison, Ref. [4] demonstrates clearly that density turbulence in the TCV SOL for all plasma conditions that can be accessed by the probe diagnostic conforms closely to Gamma distributed statistics. A further important quantity with regard to the influence of turbulent transport is the fluctuation driven radial particle flux, $\Gamma_r = n_e v_r = n_e E_{pol}/B$. Normalized experimental and code generated flux PDF's at the wall radius ($\rho = 1$) are compared in Fig. 5. In both cases the flux distribution is highly skewed with most events propagating outwards. Agreement between code and experiment is extremely encouraging.

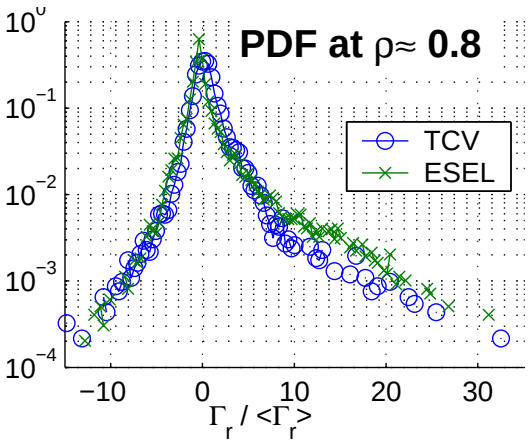

Figure 5: Comparison Γ_r-PDF from the ESEL model with experiment.

Conclusion

The salient features of intermittent density fluctuations in the SOL of TCV [4] have been reproduced in dedicated simulations using a 2D fluid model [3]. The density statistics of both simulation and TCV data conform closely to a single stochastic process, namely the Gamma process, in the entire SOL and also far into the shadow region. Such model-experiment agreement essentially validates the picture of radially propagating blobs dominating cross field transport in the SOL. Furthermore, the observation that detailed statistical characterization of the intermittency is so well matched by simulations indicates that anomalous transport in the tokamak SOL is dominated by 2D interchange turbulence.

Acknowledgement: The authors thank M. Wischmeier and S. Mueller for fruitful discussions. This work was partly funded by the Fonds National Suisse de la Recherche Scientifique and by the Danish Center for Scientific Computing through grants CPU-1101-08 and CPU 1002-17.

References

[1] D. Bohm, The characteristics of electrical discharges in magnetic fields, McGraw-Hill New York, 1949

[2] R. J. Goldston and P. H. Rutherford, Introduction to plasma physics, Bristol: Institute of Physics Publishing, 1997

[3] O.E. Garcia *et al*, Phys. Plasmas **12**, 062309 (2005)

[4] J. Horacek, R.A. Pitts and J.P. Graves, Czechoslovak Journal of Physics **55**, 271 (2005); J.P. Graves, J. Horacek, R.A. Pitts and K.I. Hopcraft, Plasma Physics and Controlled Fusion **47**, L1-L9 (2005)

[5] M. Evans, N. Hastings, B. Peacock, Statistical distributions, ISBN 0-471-55951-2, John Wiley & sons, Inc., 1993

[6] F. Sattin *et al*, Physics of Plasmas,**11** (2004), 5032

[7] E.J. Gumbel, The Statistics of Nature, New York: Columbia University Press, 1958

[8] S.T. Bramwell, P.C.W. Holdsworth and J-F. Pinton, Nature, **396** (1998), 552

[9] van B.P. Milligen *et al*, Physics of Plasmas **12** (2005), 5, 052507